Improved Charge Transfer at Carbon Nanotube Electrodes**

By *Pichumani J. Britto*, *Kalathur S. V. Santhanam*, *Angel Rubio*, *Julio A. Alonso*, and *Pulickel M. Ajayan**

The closed topology and tubular structure of carbon nanotubes[1–3] make them unique among different carbon forms and provide pathways for chemical studies. A number of investigations[4–8] have been carried out to find applications of nanotubes in catalysis, hydrogen storage, intercalation, etc. Since carbon-electrode-based fuel cells have been experimented with for decades, it is of importance to learn the electrodic performance of these new carbon structures. We report here results of the electrocatalytic reduction of dissolved oxygen (important H_2–O_2 fuel cell reaction), using microelectrodes constructed from multiwalled nanotubes. In parallel, ab initio calculations were performed for oxygen deposited on the lattice and defect sites[9] of nanotube surfaces to determine the charge transfer during oxygen reduction and compared with similar reactions on planar graphite.

The microelectrodes were constructed in the following way (see Fig. 1). Multiwalled nanotubes (10 mg) prepared by the electric arc discharge process[3] and liquid paraffin (4 μL) were intimately mixed, placed in the narrow cylindrical slot of a Perspex holder and then packed by smooth vibration. The assembly was cured at 50 °C for 30 min. From the inner side of the Perspex, contact to a copper lead was made through conducting paint. Carbon paste electrodes (based on commercially available graphite powder) were prepared similarly. Carbon nanotube electrodes were prepared earlier by similar techniques to probe bioelectrochemical reactions.[8]

The need for oxygen reduction at catalytic surfaces has been recognized in fuel cells, batteries, and many other electrodic applications.[10–16] Hence, oxygen reduction at nanotube surfaces is of great interest. Electrochemical reduction of dissolved oxygen is carried out in aqueous acidic (H_2SO_4) and neutral media (1 M KNO_3). The solution is first degassed by bubbling nitrogen gas for about 15–30 min in order to record the background current–voltage curves. Under these conditions, no cyclic voltammetric peak in the potential range 0 to –0.8 V were observed. The same solutions were then saturated with oxygen by bubbling oxygen gas for 15 min. The cyclic voltammetric curve showed a well-defined peak at E_{pc} = –0.31 V vs. SCE (saturated calomel electrode) in H_2SO_4 solution (pH 2) at the carbon nanotube electrodes. At the carbon paste electrodes only an ill-defined peak is seen at E_{pc} = –0.48 V. In the KNO_3 medium (pH 6.2), the reduction of dissolved oxygen is observed at E_{pc} = –0.51 V at the carbon nanotube electrode. This peak is shifted at the carbon paste electrode by about 30 mV. The shift of the peaks, corresponding to the reaction on the nanotube electrodes, is a strong indication of the electrocatalysis on this electrode (see discussion below). The shift may be considered as an overpotential, which indicates a more facile reaction occurring at the nanotubes compared to other carbons. The electrochemical reduction of oxygen is a function of pH of the medium[10,11] as proton participation occurs as described by Equation 1.

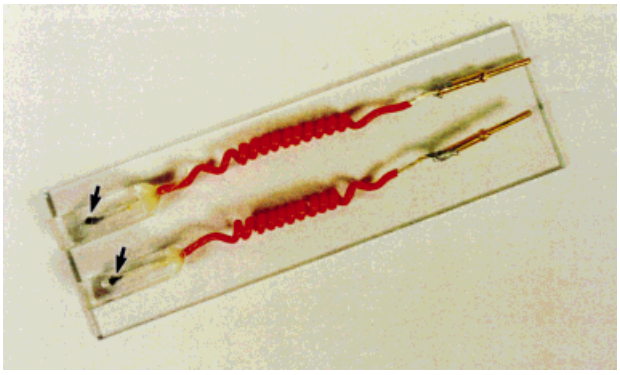

Fig. 1. Construction of a carbon nanotube microelectrode. The three main parts are the copper lead, the Perspex holder, and the slot in it, which contains packed nanotubes (seen as a black spot, pointed out by the arrows). The connection between the lead and nanotubes is through conducting adhesive paint. The black spot on the holder acts as the nanotube electrode.

$$O_2 + 2e^- + 2H^+ \longrightarrow H_2O_2 \qquad (1)$$

This reaction has been well discussed in literature.[10] The reduction potential of oxygen will shift the pH of the solution due to Reaction 1. The reduction at a metal cathode proceeds through its dissociative adsorption. The peroxide formation is a consequence of the differences in the rate of electron transfer and in the rate of oxygen dissociation to adsorbed oxygen atoms. Peroxide can then be formed as a suitable intermediate. Oxygen therefore undergoes a $2e^-$ reduction. However, if the oxygen reduction proceeds through a superoxide ion and a subsequent protonation, as

[*] Dr. P. M. Ajayan
Department of Materials Science & Engineering
Rensselaer Polytechnic Institute
Troy, NY 12180-3590 (USA)
Dr. P. J. Britto
Chemical Physics Division, Tata Institute of Fundamental Research
Homi Bhabha Road, Mumbai 400 005 (India)
Dr. K. S. V. Santhanam
Department of Chemistry
Rochester Institute of Technology
Rochester, NY 14623 (USA)
Dr. A. Rubio, Dr. J. A. Alonso
Departamento de Fisica Teorica, Universidad de Valladolid
E-47011 Valladolid (Spain)

[**] A.R. and J.A.A. acknowledge partial support from DGES Grant No. PB-95-0720-C02-01 and PB95-0202 and European Community TMR Contract No. ERBFMRX-CT96-0067 (DG12-MIHT). Computer time was provided by C4 (Centre de Computacio i Comunicacions de Catalunya). We have benefited from very fruitful discussions with Prof. J. Soler concerning the simulations and graphics program. P.M.A acknowledges support from the DMR division of the National Science Foundation for work on carbon nanotubes through the CAREER grant.

  0935-9648/99/0201-0154 $ 17.50+.50/0

ADVANCED MATERIALS

in Equation 2, the reduction potential can reach a value of –0.13 V (vs. SCE).

$$\{O_2 + e^- \longrightarrow O_2^-\,;\, O_2^- + HA \longrightarrow HO_2 + A^-\} \qquad (2)$$

The reduction potential of $HO_2 + e^- \longrightarrow HO_2^-$ is estimated as –0.74 from the free energy data.[10] The cyclic voltammetry of oxygen cannot be used to estimate the true reduction potential of oxygen as it is an irreversible process where O_2/O_2^- and O_2^-/HO_2^- are not in equilibrium. However, the cyclic voltammetric wave reflects the charge transfer rates for the reduction of oxygen.

The deposition of metals such as Pd and Ag onto carbon nanotubes significantly shifts the above peaks anodically. With 4.5 μg/cm^2 of Pd deposited on the carbon nanotube electrode, the cyclic voltammetric peak potential E_{pc} is shifted to 0.07 V (in 1 M H_2SO_4). A much smaller shift is observed at the carbon paste electrode. The polarization curves at the carbon nanotube electrodes were recorded at a sweep rate of 2 mV/s with dissolved oxygen constantly being bubbled into the medium. Tafel plots were constructed following the established procedures.[10,11] Results of the electrocatalysis of the above reaction using nanotube catalysts are summarized in Table 1. The exchange current densities shown are indications of how fast the reaction is taking place. The values for the current density in the acidic medium are compared for nanotubes, carbon paste and a commercial fuel cell catalyst (Pt/C/Nafion). For the latter, values are lower since resistances are cumulative when supported by Nafion or other membranes, and hence are not directly comparable to the results here.[17] Since the surface topology of the nanotubes can vary, the true active surface area (for current density determination) is estimated electrochemically, from the current–voltage curves and chronoamperometric recordings.[19] We focus on the comparison between nanotubes and graphite, and the values of the current densities, which are at least five times higher for nanotubes (the trend is similar in acidic and neutral media). Figure 2 shows the cyclic voltammetric curves for the first reduction of oxygen at the nanotube electrode, in acid medium, being compared to the same for carbon paste electrodes under similar conditions.[20] The peak current at the nanotube electrode increases with sweep rate and follows the diffusion-controlled process. The second reduction peak of oxygen is situated beyond the first peak before the background limit. At this stage, oxygen reduction proceeds to water by a four-electron process. At the carbon paste electrode these peaks are shifted towards more negative potentials and are ill defined. Also note that the background curve at the carbon nanotube electrode is shifted anodically compared to the carbon paste electrode. The diffusion coefficient of oxygen in the reaction is determined (using potential step electrolysis at –0.6 V) to be 3.1×10^{-5} cm^2/s compared to a similar reported literature value of 2.6×10^{-5} cm^2/s.[21] We have also studied metal (e.g., Ag, Pd) deposited nanotube electrodes and preliminary data suggest that the exchange currents at metal/nanotube electrodes are much higher than those observed for metals on graphite or glassy carbon electrodes. The latter systems have been tested extensively for improved electrodic performance of fuel cells.[18] Very recently, pyrolitic nanotube membranes made using ceramic templates and deposited with metal catalysts have been reported to catalyze the oxygen reduction reaction.[22]

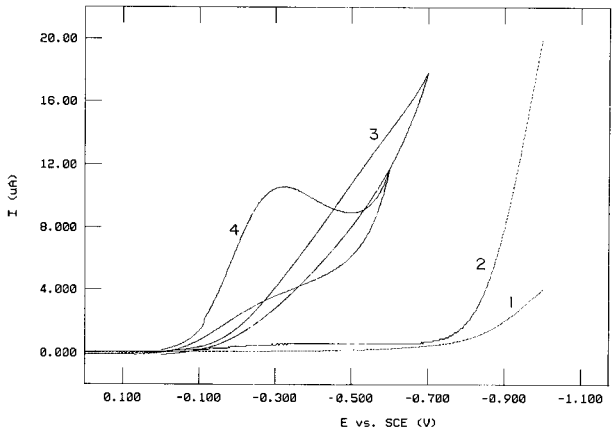

Fig. 2. Current–voltage curves for the electrocatalysis of dissolved oxygen at carbon nanotube and carbon paste electrodes. Medium is H_2SO_4 (pH 2): 1) background with carbon paste (no oxygen); 2) background with carbon nanotubes (no oxygen); 3) with dissolved oxygen (~1 mM) at the carbon paste; 4) with dissolved oxygen (~1 mM) at the nanotubes. The recordings were all done at a sweep rate of 100 mV/s.

Table 1. Comparative data for the electrocatalysis of oxygen reduction at carbon nanotubes and graphite paste electrodes in acidic and neutral media. i_o is obtained from the intercept of the overpotential vs. log (current density) plot. It represents the rate constant for the electron transfer process. The values reported are all for room temperature and averages from several experiments. The first three values are from the present work whereas the last [17] is a literature value [18].

Electrode reference material	Exchange current density i_0 [A/cm^2]
Carbon nanotubes H_2SO_4 (pH 2)	6.3×10^{-4}
Graphite H_2SO_4 (pH 2)	1.2×10^{-4}
Carbon nanotubes/Pd (0.08 mg/cm^2) H_2SO_4 (pH 2)	36.6
Pt/C/Nafion (Commercial)	1.09×10^{-7}

To understand the microscopic mechanism of electron transfer on nanotubes, we performed ab initio density-functional-theory calculations and molecular dynamics (MD) simulations. Here we discuss the adsorptive dissociation of oxygen on the carbon nanotube surface and the charge transfer process, concentrating on Reaction 1 given above. A complete understanding of the former needs a more detailed study concerning the activation energies and the rates of dissociation. However, assuming that the dissociation of the O_2 molecule takes place (preliminary MD simulations suggest this), we look for the minimum energy of a single atom located close to the regular lattice sites (hexa-

  0935-9648/99/0201-0155 $ 17.50+.50/0

gons) and defects (pentagons and heptagons) on the nanotube surface. Then we compute the trapping of electrons by the oxygen atom on the tube-wall surface, which subsequently leads to the interaction of the negatively charged atoms with protons to form H_2O_2.

We describe the interaction between valence electrons and ionic cores by non-local norm-conserving pseudopotentials for C and O[23] with a 60 Ry energy cutoff for the plane-wave expansion of the wavefunctions. We work within periodic boundary conditions by keeping the minimum distance between tubes (or sheets) as 5.5 Å to ensure negligible interaction. The ground-state geometry is obtained by minimizing the Hellmann–Feynman forces. The computed C−C and C−O bond lengths for graphite and C_{60} structures (1.42, 1.40, and 1.46 Å, respectively) and molecules (C-dimer, CO and CO_2) agree with experimental values within 1 %. The forces acting on the atoms are derived from the corresponding electronic ground state, which is accurately described within the local-spin-density approximation. Since only the outermost layer of the nanotube takes part in the charge transfer, a comparison between experimental work on multishell tubes and calculations on single-walled (SW) nanotubes is deemed appropriate. Calculations also show that the effect of curvature is minimal.

As a first step, we determined the static ($T = 0$) equilibrium atomic positions and the corresponding Mulliken population analysis for a single oxygen atom impurity sitting on a perfect and defective graphene sheet and a SW nanotube for various initial positions: hexagonal sites and defects (pentagons and heptagons). We used a basis set of localized 2s–2p pseudoatom orbitals for C and O in order to carry out the Mulliken orbital populations analysis (atomic and bond charges are easily obtained in this basis set representation). Within this scheme we have a consistent and accurate way of comparing the charge transfer to the oxygen atom in different environments, although the absolute values are not representative of the formal oxidation number.

In Figure 3a we show a typical bond-rotation defect of a (6,6) SW carbon nanotube[24] and the corresponding simulated three-dimensional local density of states[25] for occupied states close to the Fermi level. All nanotubes were relaxed to their equilibrium geometries before oxygen approached them. The calculations for a closed (6,6) carbon tube were performed on tubular nanotube sections terminated on one side by H atoms that saturate the bonding of the two-coordinated C-atoms, and on the other side by fullerene-like caps with a six-fold rotation symmetry (Fig. 3b). It is clearly seen that due to the higher density of states at the pentagonal sites, these would act as electrophilic reaction sites. The same behavior is obtained at the nanotube tips and nanoparticles where pentagons are present.[26] Oxygen reduction with a larger charge transfer takes place at these high density of states sites. The analysis of the Mulliken partition shows an ionic local environment for the oxygen atom. We take as reference the charge

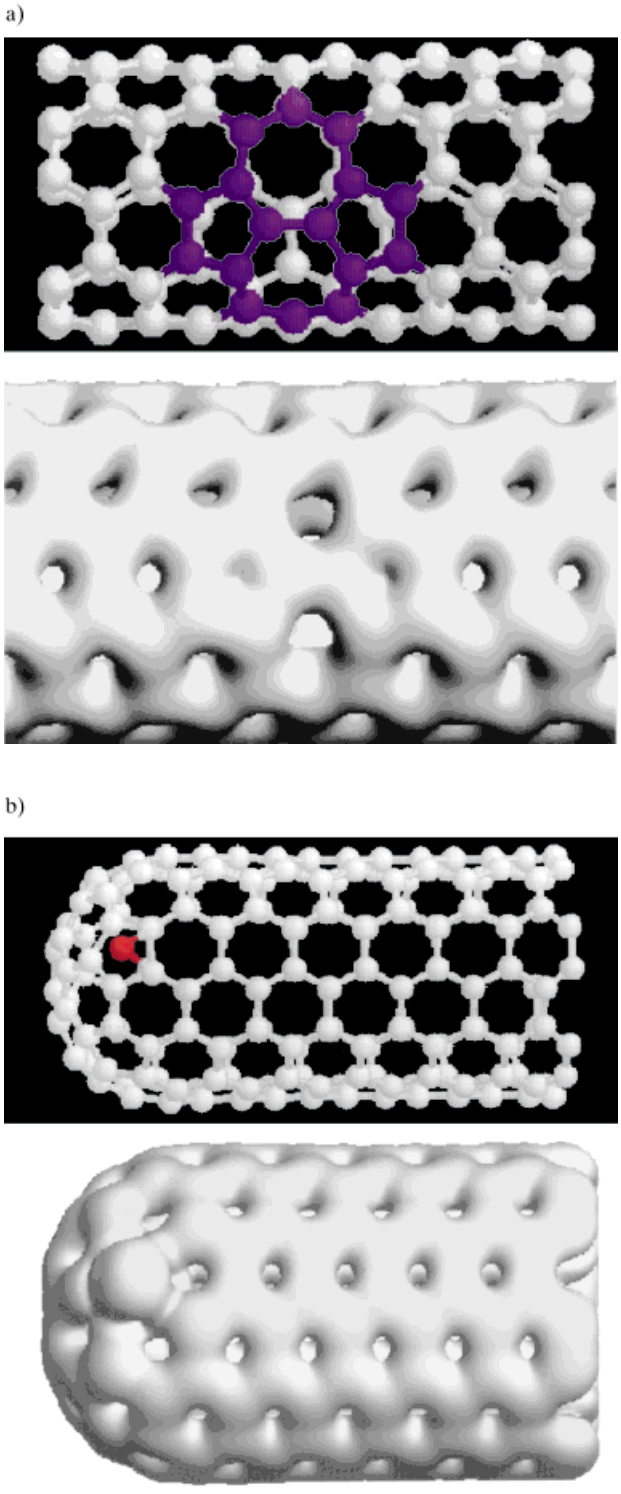

Fig. 3. a) Top: Ball and stick model for a single-walled nanotube (6,6) with a bond-rotation defect (two 5-7 pairs) (blue atoms in the structure). Bottom: Corresponding simulated 3D local density of states image of occupied orbitals around the Fermi level for this tube. We see an increase in the available density of states at the pentagonal sites with respect to the other hexagonal or heptagonal sites. This establishes an enhanced oxygen reduction site for the charge transfer reaction. b) Same as (a) but for an oxygen atom on a nanotube tip. High density of states sites indicate preferential sites for the reduction reaction.

  0935-9648/99/0201-0156 $ 17.50+.50/0

ADVANCED MATERIALS

transfer for a perfect graphene sheet. For the SW nanotubes, the calculations show that curvature leads to a slightly larger charge transfer that tends as $1/D$ (D is tube diameter) to the graphitic values (2 % larger for the (6,6) nanotube with D = 0.82 nm). This slight increase is attributed to curvature-induced σ–π hybridization that alters the energy band dispersion close to the Fermi level.[27] The average Mulliken population at a pentagon is 3–4 times larger than at a graphene hexagon in both planar and tubular structures. Furthermore, the computed distance between negatively charged oxygen and the closest surface carbon atom on the nanotube (~1.8 Å) is larger than any molecular C–O bond length, indicating the lack of bond formation between carbon and oxygen. Atomic oxygen preferentially sits on the defect sites, producing a region with very large local density of states (Fig. 3b) that could be easily reduced by protons in the solution.

We have performed room temperature MD simulations for the deposition of an O_2 molecule on a defective graphite sheet in order to assess the reliability of the single atom model described here. The main result is the fact that the O_2 molecule acquires a negative charge on approaching the surface, then stays on the surface and after some picoseconds starts slowly to dissociate. Also, the first indication is that the defects tend to activate the dissociation of the O_2 molecule. This validates oxygen reduction taking place through charge transfer to atomic oxygen, which is an intermediate transition state for the negatively charged oxygen species.

The calculations indicate that pentagons at the nanotube tips, pentagon–heptagon defect pairs in the lattice, and, to a lesser extent, curvature are responsible for the improved activation behavior of oxygen reduction. It has been seen that surfaces of as-grown multiwalled nanotubes contain large numbers of defects, which are removed only by high temperature annealing treatment.[3] The improved catalytic behavior of nanotube electrodes was evidenced previously in bio-electrochemical studies.[8] Our new results here confirm the potential of using nanotubes in electrodic applications such as fuel cells. The low density of nanotubes should be an added advantage in these applications.

Received: June 22, 1998
Final version: September 14, 1998

[1] S. Iijima, *Nature* **1991**, *354*, 56.
[2] M. S. Dresselhaus, G. Dresselhaus, P. C. Eklund, *Science of Fullerenes and Carbon Nanotubes*, Academic Press, New York **1996**.
[3] T. W. Ebbesen, *Carbon Nanotubes: Preparation and Properties*, CRC Press, Boca Raton, FL **1997**, pp. 225–248.
[4] A. C. Dillon, K. M. Jones, T. A. Bekkedahl, C. H. Kiang, D. S. Bethune, M. J. Heben, *Nature* **1997**, *386*, 377.
[5] V. Z. Mordkovich, M. Bazendale, R. P. H. Chang, S. Yoshimura, Synth. Met. **1997,** *86*, 2049.
[6] C. Niu, E. K. Sichel, R. Hoch, D. Moy, H. Tennet, *Appl. Phys. Lett.* **1997**, *70*, 1480.
[7] J. M. Planeix, N. Coustel, B. Coq, V. Brotons, P. S. Kumbhar, R. Dutartre, P. Geneste, P. Bernier, P. M. Ajayan, *J. Am. Chem. Soc.* **1994**, *116*, 7935.
[8] P. J. Britto, K. S. V. Santhanam, P. M. Ajayan, *Bioelectrochem. Bioenerg.* **1996,** *41*, 121. J. J. Davis, R. J. Coles, A. O. H. Allen, *J. Electroanal. Chem*. **1997**, *440*, 279.
[9] V. H. Crespi, M. L. Cohen, A. Rubio, *Phys. Rev. Lett*. **1997**, *79*, 2093.
[10] J. O. M. Bockris, S. Srinivasan, *Fuel Cells*, McGraw-Hill, New York **1969**. A. McDougall, *Fuel Cells*, Macmillan, London **1976**.
[11] A. J. Bard, L. R. Faulkner, *Electrochemical Methods*, Wiley, New York **1980**.
[12] J. Ge, D. C. Johnson, *J. Electrochem. Soc.* **1995**, *142*, 3420.
[13] T. E. Mallouk, *Nature* **1990**, *343*, 515.
[14] M. Uchida, Y. Aoyama, A. Ohta, *J. Electrochem. Soc.* **1995**, *142*, 4143.
[15] A. Parthasarathy, C. R. Martin, S. Srinivasan, *J. Electrochem. Soc.* **1991**, *138*, 916.
[16] S. Srinivasan, O. A. Velev, A. Parthasarathy, D. Manko, A. J. Appleby, J. Power Sources **1991**, *36*, 299.
[17] The commercial catalyst corresponds to Pt on carbon (20 % Pt/C) with loadings of 0.4 mg/cm^2 on 125 μm Nafion Dupont membranes. The conditions for the reaction using the commercial catalyst are quite different and not comparable to experiments performed here. Commercial carbon electrodes are three-phase electrodes: gas, liquid, and solid. They typically contain a hydrophobic membrane or binder attached to the carbon electrode. Due to the limited solubility of oxygen in the medium the output current will not be high as compared to the reduction on the carbon nanotube or carbon paste electrodes as reported here, where direct molecular oxygen approach is possible. This will result in differences in the charge transfer rates and exchange current density values. The value for the commercial catalyst is merely to show the acceptable limits for operation of a commercial cell.
[18] T. Vargas, R. Varma, in *Techniques for Characterisation of Electrodes and Electrochemical Processes* (Eds: R. Varma, J. R. Selman), Wiley, Chichester **1991**, p. 717.
[19] The true active surface area used to estimate exchange current density is estimated from the current–voltage curve in cyclic voltammetry of 5 mM $K_4Fe(CN)_6$ and the chronoamperometric recordings. Using the peak current or the slope of the Cottrell's plot the area of the electrode is calculated with the diffusion coefficient of $K_4Fe(CN)_6$ as $D = 0.76 \times 10^{-5}$ cm^2/s and the number of electrons taking part in the reaction, $n = 1$ [11].
[20] R. J. Taylor, A. A. Humfray, *J. Electroanal. Chem*. **1975**, *64*, 95.
[21] I. M. Kolthoff, J. J. Lingane, *Polarography*, Vol. 2, Interscience, New York **1952**, p. 553.
[22] G. Che, B. B. Lakshmi, E. R. Fisher, C. R. Martin, *Nature* **1998**, *393*, 346.
[23] N. Troullier, J. L. Martins, *Phys. Rev. B* **1991**, *43*, 1993.
[24] We use the notation of N. Hamada, S. Sawada, A. Oshiyama, *Phys. Rev. Lett*. **1992**, *68*, 1579.
[25] The 3D local density of states is computed within an energy window of 0.8 V where we collect information from the states close to the Fermi level that are relevant for the reduction process studied here.
[26] D. L. Carroll, P. Redlich, P. M. Ajayan, J. -C. Charlier, X. Blase, A. De Vita, R. Car, *Phys. Rev. Lett*. **1997**, *78*, 2811.
[27] The curvature- (to a lesser extent) and defect-induced metallization and the edge-free structure could explain the improved charge transfer and catalysis of nanotubes, compared to other carbons.

  0935-9648/99/0201-0157 $ 17.50+.50/0